2008 20th International Lightning Detection Conference
21-23 April • Tucson, Arizona, USA
2nd International Lightning Meteorology Conference
24-25 April • Tucson, Arizona, USA

Assimilation of lightning data using a diabatic digital filter within the Rapid Update Cycle

Stephen S. Weygandt, Ming Hu, Stanley G. Benjamin, Tanya G. Smirnova,
Kevin J. Brundage, John M. Brown
NOAA Earth System Research Laboratory – Global Systems Division
Boulder, CO

1. INTRODUCTION

Driven by society's need for accurate thunderstorm prediction guidance and the ever increasing capacity of supercomputers, efforts to improve the assimilation and modeling of thunderstorms have continued to accelerate over the past decade. The efforts have included improvements to the operational models (run with horizontal resolutions of order 10 km, requiring the use of cumulus paramterizations) and to experimental models (run with resolutions of 4-km or less, explicitly resolving convective storms). A key focus for these efforts has been the data assimilation systems for the mesoscale convective environment and the direct assimilation of convective-scale data. The assimilation of convective scale date has focused primarily on the use of radar data (reflectivity and radial velocity), but awareness of the utility of lightning data as a supplementary data source has been increasing within the data assimilation community. Presently a number of efforts to assimilate lightning data are underway.

Within the NOAA Rapid-Update Cycle (RUC) model assimilation system (Benjamin et al., 2004a,b), lightning data have been used in the experimental real-time parallel runs at GSD to improve the initialization of clouds, hydrometeors, and convection. After initially experimenting with direct modification of hydrometeors using radar reflectivity and lightning data, in 2007 we switched to a new technique in which reflectivity and lighting data are used to create a latent heating-based temperature tendency field, which is applied during a pre-forecast diabatic digital filter initialization.

Developmental work is ongoing to replace the current RUC with a new hourly cycled mesoscale assimilation system known as the Rapid Refresh (RR). The RR domain will cover all of North America and adjacent waters, with a considerable portion of the domain not covered by a radar network. Thus, the value of lightning data for the RR (including networks from Alaska, Canada and long range data covering Mexico and the Pacific and Atlantic oceans) is significant. Fig. 1 shows the expanded Rapid Refresh domain, as well the current RUC domain and an experimental 3-km nested domain, known as the High Resolution Rapid Refresh (HRRR). The HRRR is a prototype for a potential future operational CONUS explicit convection resolving forecast system. The HRRR is currently nested within the RUC, and the benefits from the radar / lightning assimilation within the RUC also improve the HRRR forecasts. The HRRR nest will be migrated to the RR and benefit from a similar assimilation system within the RR. Ultimately the HRRR will have its own storm-scale assimilation system.

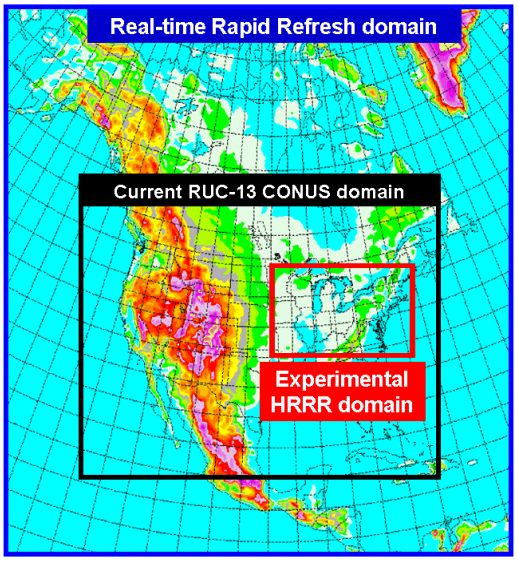

Fig. 1. Diagram showing the horizontal domains of the current NCEP operational 13-km hourly cycled RUC model, real-time 13-km Rapid Refresh domain currently running with a 1-h cycle at GSD (and scheduled to replace the RUC at NCEP in 2009-2010), and the experimental 3-km High Resolution Rapid Refresh domain currently running hourly at GSD.

The RUC radar / lightning assimilation technique has been ported to the Gridpoint Statistical Interpolation (GSI) analysis package (developed by NCEP) that is being used to

* *Corresponding author address:* Steve Weygandt, NOAA/GSD, R/E/GSD, 325 Broadway, Boulder, CO 80305, Stephen.weygandt@noaa.gov

initialize the Rapid Refresh (Hu et al. 2008) and work to evaluate the performance of the assimilation procedure with and without lighting data is proceeding for both RUC and the RR model systems. We currently have access to NLDN data over CONUS and BLM lightning data over Alaska. As shown in Fig. 2, the Alaskan data provide crucial information across a large radar data void region and will be especially helpful during the Alaskan summer fire season. These data will be used to more fully evaluate the procedure over the Alaskan region during summer 2008.

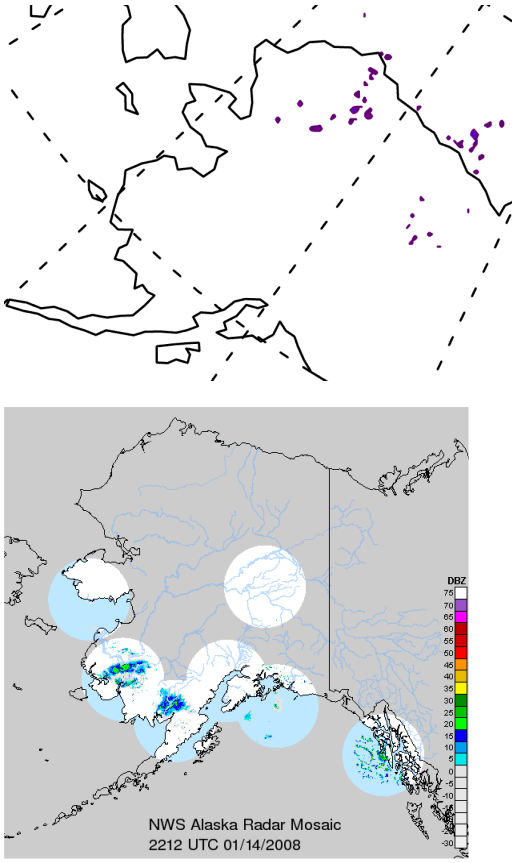

Fig. 2 (top) Lightning ground stroke density for 00z 10 July 2008 over Alaska. Information from BLM data provided by the Alaskan Region National weather Service. (bottom) Map showing low-level radar data coverage circles for the Alaskan WSR-88D radar network. Note, actual radar echoes are not time/date-matched with the lightning data and higher-level scans provide somewhat larger coverage

In this paper, we will first describe the combined lighting / reflectivity assimilation procedure (including some new results the concerning lightning – reflectivity relationship), then show some 13-km and 3-km results from use of technique ***using primarily reflectivity data.*** While the lighting data will be extremely beneficial in regions with no radar coverage and may also be very helpful in areas with radar data coverage, we have not yet completed experiments to the impact solely due to the lightning data. We will conclude with a summary of our plans for future work.

2. COMBINED LIGHTNING / REFLECTIVITY ASSIMILATION SYSTEM

The combined reflectivity / lighting assimilation procedure (depicted in Fig. 3) is now described for the RUC model system. These components are being transferred to the Rapid Refresh system. The radar / lightning ingest and cloud analysis portion has been fully transferred and the diabatic digital filter is now working in the RR model core (WRF ARW). Work to couple the components will be completed later this year, providing the RR with a reflectivity / lighting assimilation capability similar to that in the GSD RUC.

The Rapid Update Cycle (Benjamin et al. 2004a,c; 2006; 2007) is an hourly updated mesoscale analysis and prediction system running operationally at the National Centers for Environmental Prediction (NCEP). RUC prediction grids are used heavily as mesoscale guidance for short-range forecasts, especially by aviation, severe weather, and situational awareness forecast users. The RUC model utilizes a hybrid sigma-isentropic vertical coordinate, and includes prognostic equations for five cloud and precipitation species (following Thompson, 2004). Within the hourly RUC 3DVAR (Benjamin et al 2004c, Devenyi and Benjamin 2003) analysis, a large variety of observations are blended with the previous 1-h RUC forecast to update the mass, velocity and moisture fields. Inertial-gravity wave energy excited by the hourly assimilation is controlled by the use of a diabatic (since 2006) digital filter (Lynch and Huang 1992, Huang and Lynch 1993) within the RUC model. As illustrated in Fig. 3, the digital filter includes a backward adiabatic integration followed by a weighted averaging, then a forward diabatic integration followed by a second weighted averaging to obtain a more balanced set of model initial fields.

The RUC 3DVAR analysis is complemented by a non-variational cloud analysis (Benjamin et al. 2004b, Weygandt et

al. 2006a,b) in which cloud- and precipitation-related observations (METAR, satellite, radar, and lightning) are combined and used to modify the cycled cloud and precipitation fields. Hu et al. (2008) describe recently completed work to build a generalized cloud analysis within the GSI (including contributions from the RUC and ARPS cloud analyses).

The new RUC radar reflectivity / lightning assimilation procedure utilizes two existing RUC system components, the cloud analysis and the diabatic digital filter initialization (DDFI), to prescribe during the pre-forecast integration a specified temperature tendency (warming) within the radar-observed reflectivity regions. This temperature tendency is deduced as a latent heating rate from the radar-observed reflectivity and lightning data within the cloud analysis. Then, during the diabatic forward model integration portion of the digital filter (and within the radar reflectivity region) the model-calculated temperature tendencies from the explicit microphysics scheme and cumulus parameterization are replaced by the temperature tendency derived from the radar reflectivity data. Fig. 3 provides a schematic that illustrates the application of the latent heating based temperature tendency during the forward model portion of the DDFI. The diagnosis of the latent heating rate from the 3D radar mosaic and the NLDN data occurs within the RUC cloud analysis. First lightning ground stroke densities are used to supplement the reflectivity via a simple empirical formula. Then a latent heating rate proportional to the reflectivity intensity is found.

Information about the reflectivity and lightning data sources is as follows. The radar reflectivity used in the cloud analysis is from the NSSL national (CONUS) 3D radar mosaic grid with a 1-km horizontal resolution over 30 vertical levels and a 5-minute update cycle (Zhang et al. 2006). The data are generated by combining base level data from all available radars, performing quality control, and then combining reflectivity observations from individual radars onto a unified 3D Cartesian grid. The lightning ground stroke data is from the National Lightning Detection Network (NLDN) and can provide thunderstorm information in areas without radar coverage.

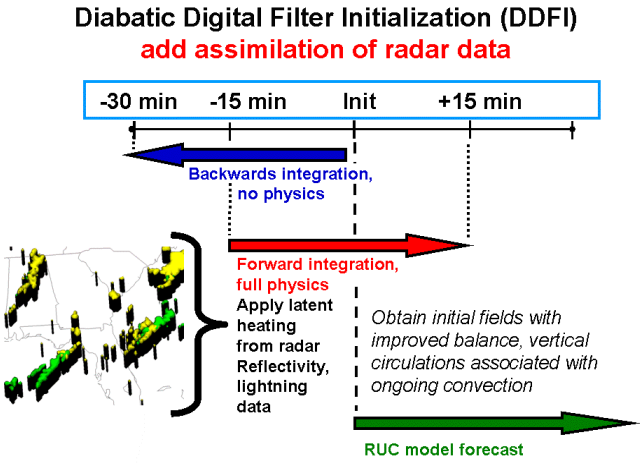

Fig. 3. Schematic diagram illustrating the application of the radar reflectivity-based latent heating within the diabatic digital filter initialization within the RUC model. In the sample plot, yellow and green shading show the contributions from the reflectivity and lightning data, respectively.

The lightning data are converted to reflectivity data using a very simple assumed relationship between flash density within a given RUC grid box and grid box average reflectivity. This relationship is given by:

$$\mathbf{REFL = min\ [\ 40,\ 15 + (2.5)(LTG)]},$$

Where LTG is the number of lighting flashes in a given RUC grid box summed over a 40 minute period around the analysis hour (-30 min. to + 10 min.) and REFL is the derived proxy reflectivity in dBZ. The proxy reflectivity is then used to supplement the NSSL reflectivity mosaic in columns where the lighting derived proxy reflectivity exceeds the NSSL reflectivity. Initially a simple sinusoidal distribution in the vertical has been assumed for the proxy reflectivity. Section 3 described some recent work to obtain a statistical lighting – reflectivity (L-R) relationship and vertical distribution function.

The RUC radar-enhanced DDFI method for initializing ongoing precipitation systems has a number of positive attributes. First, the method modifies the wind fields in a manner roughly consistent with the ongoing convection. Given the limitations of the observations, the horizontal grid resolution, and the parameterized representation of the convection, this is an appropriate objective. Numerous studies have shown that without modifying the wind field in this manner, the

model retention of any assimilated hydrometeor information is short-lived.

Second, the modification of the wind field is done in a manner that minimizes shock to the model. Rather, the wind field evolves gradually during the DDFI to the prescribed heating rate. Note that the associated drying that would result is offset by increasing the water vapor in the reflectivity region within the cloud analysis. Third, the assimilation procedure requires no additional computer time, because the diabatic digital filter is already used to control noise in the RUC model initialization.

In addition to using the reflectivity and lighting data to prescribe latent heating temperature tendencies, radar reflectivity information is used to suppress model convection in areas with no echoes. In applying this convective suppression, it is extremely important to distinguish between regions with no echo and regions with no radar coverage. In these no coverage regions, the radar data cannot determine whether precipitation systems are ongoing and convective suppression is not warranted. The application of the convection suppression is as follows:

1) Determine a 2D "no echo" region, at least 100 km from any existing echo and excluding regions with no radar coverage.
2) During the DDFI and for the first 30 minutes of the model forecast, force a convective inhibition threshold condition that precludes the calling of the cumulus parameterization routine.

3. A statistical L-R relationship

We have recently begun to evaluate the statistical relationship between the number of flashes per Rapid Refresh model grid column and the corresponding column maximum of grid averaged NSSL reflectivity. Fig. 4 shows the relationship obtained for CONUS average over a five-hour period from a cold season case early in 2008. While very preliminary, these data show a reasonable agreement with the assumed linear relationship. We will continue to evaluate this relationship over more cases and weather regimes, with a goal of replacing the simple linear relationship with a better statistically derived relationship. This preliminary statistical relationship between lightning flashes per grid column and column maximum reflectivity is complemented by a set of statistical relationships between column maximum reflectivity and vertical reflectivity profile. Using the same lightning and reflectivity observations, a set of vertical reflectivity profile curves (as a function maximum reflectivity) have been obtained. These are shown in Fig. 5., where each curve represents a different 5 dBZ bin of maximum reflectivity. Thus, with these two sets of relationships, the lighting flash rate can first be mapped to a column maximum proxy reflectivity, then to a vertical distribution of proxy reflectivity. We have not yet implemented this procedure, but will continue to evaluate this technique for mapping the lightning data to proxy reflectivity data. A related benefit of the curves in Fig 5 is a statistical basis for downward extrapolation of radar data to regions below the lowest radar scan.

Even with the simple linear L-R relationship, comparison of proxy reflectivity (derived from NLDN lighting data) and NSSL reflectivity mosaic data indicates a good agreement (subject to the imposed reflectivity limits from the assumed L-R relationship). This can be seen in Fig. 6

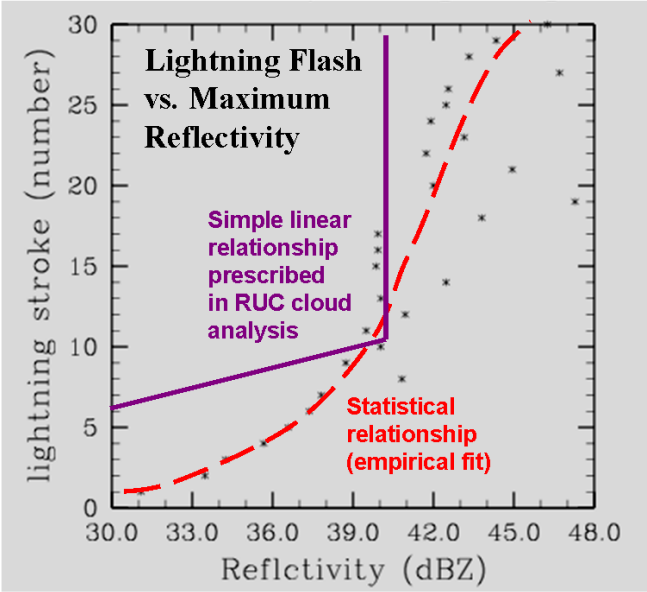

*Fig. 4. Relationship between the number of NLDN lightning flashes per Rapid Refresh grid box column and grid averaged column maximum NSSL reflectivity (dBZ). * indicate the relationship calculated from the data and the red dashed line indicates a crude fit to the point. The purple solid line depicts the assumed simple linear fit.*

4. Preliminary test case results

The coding and testing of the diabatic digital filter (without the radar assimilation) was completed in early 2006 and implemented in the NCEP operational RUC in June 2006, replacing the adiabatic DFI used since 1998. The code to process the mosaic reflectivity data (interpolate the data to the RUC grid and calculate the latent heat-based temperature tendency) and apply the temperature tendency within the DDFI was completed late in 2006, and preliminary off-line testing began in January 2007. We show here results from a simple squall-line case from 00z 8 Jan 2007, in which the analysis and forecast with and without the radar assimilation are compared. It is important to note that for this case, the radar assimilation is applied at a single analysis time, so the impact is less than can be expected when the radar assimilation is applied each hour within an evolving cycled analysis/forecast system.

Fig. 7a shows the 3-km NSSL radar reflectivity mosaic depiction of a precipitation system from 00z 8 January 2007, including a broad area of moderate radar echoes across the Mid-Atlantic States and a squall line stretching across the southeastern states. The latent heating derived from the radar reflectivity data is shown in Fig. 7b (plotted on the k= 15 RUC vertical level). The latent heating rate is plotted in deg. per 15 min with a maximum of ~ 5 K per 15 min. For this test, the heating was set proportional to the reflectivity as opposed to a reflectivity change from the background (resulting in only warming).

As expected, the application of the latent heating-based temperature tendency within the DDFI (in place of the heating from the microphysical and cumulus schemes) produces a local positive temperature anomaly and induces an associated vertical circulation, with low-level convergence and upper-level divergence. Evidence of the vertical circulation can be seen in Fig. 8, which shows the difference in the west-to-east component of the wind for the experimental analysis (with the radar assimilation) relative to the control analysis (without the radar assimilation) for 2 different model levels. At low-levels (K = 15, shown Fig. 8a) the couplet of velocity

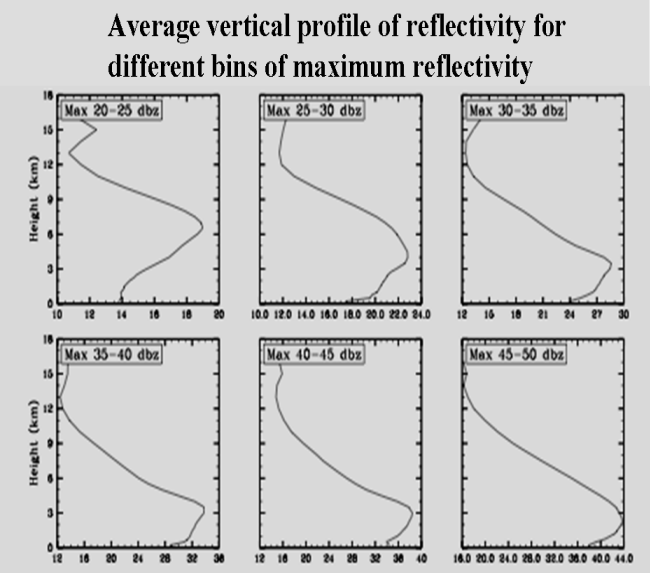

Fig. 5. Average vertical profile of reflectivity as a function the column maximum reflectivity. The variation of the vertical profile can be seen as column maximum reflectivity increases (in 5 dBZ bins) from 20-25 dBZ through 45-50 dBZ. The curves were derived from 5 h of CONUS data from a cold season case in early 2008.

differences clearly shows convergence along the squall-line. Conversely, at upper-levels (K=35, shown in Fig. 8b), a broader area of divergence is seen.

The impact of the radar data assimilation is quite evident in the resultant short-range precipitation forecast. Fig. 9 illustrates the difference between the control and radar assimilation experiment for the 1-h forecast of 15 min. accumulated total (explicit + parameterized) precipitation (45 to 60 min.). Whereas the control experiment predicts very little precipitation along the squall-line (Fig. 9a), the radar assimilation forecast produces significant precipitation along the squall line (Fig. 9b). Further examination of the precipitation fields (not shown) indicates the radar assimilation projects onto both the parameterized and grid-scale precipitation schemes within the RUC model. Forecast differences are also evident at 2 hours as shown in Fig. 10.

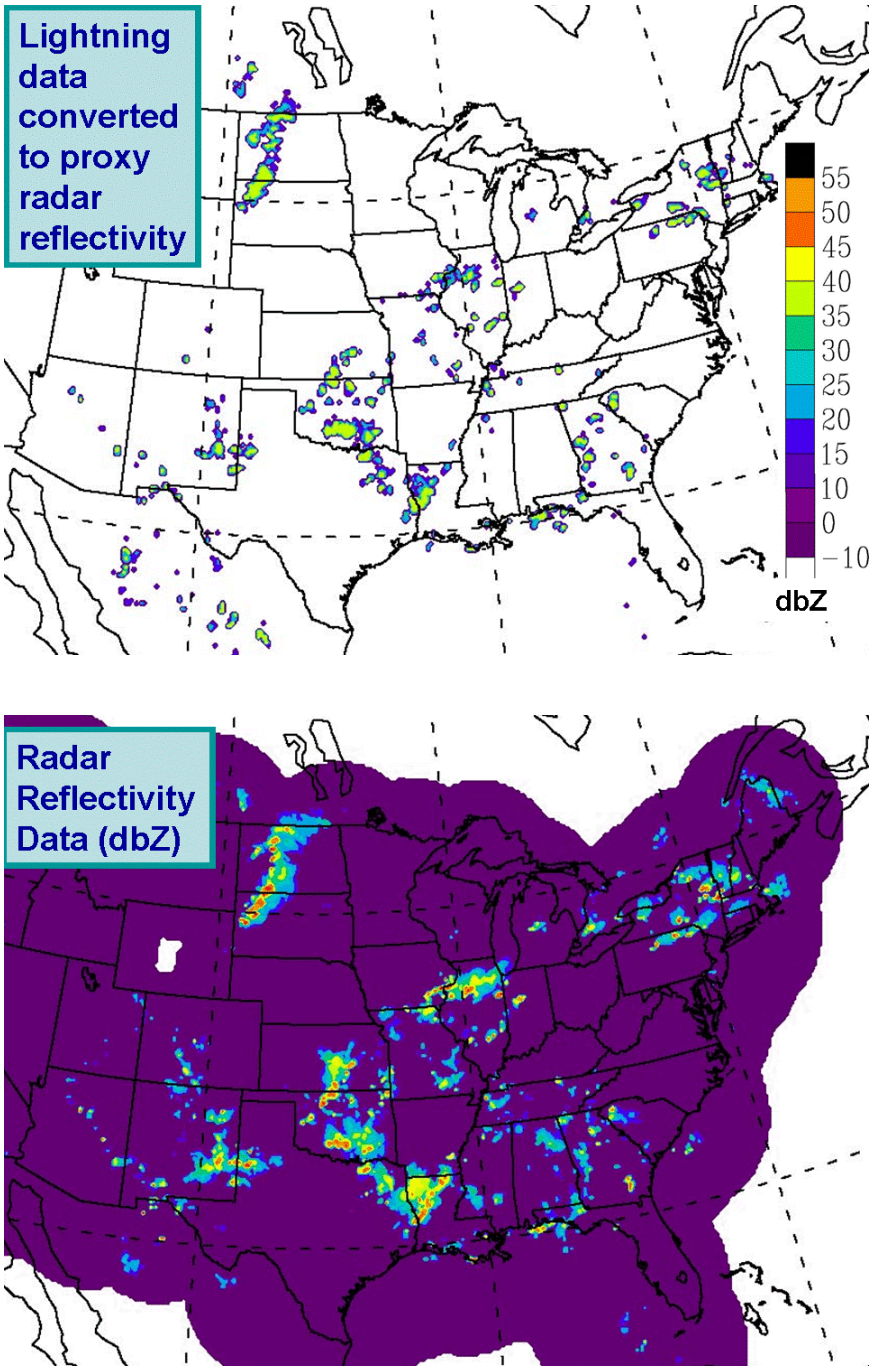

Fig. 6. Comparison of (top panel) proxy reflectivity (converted from NLDN lightning flashes per grib box using the simple linear relationship) and (bottom panel) grid box average radar reflectivity field from NSSL reflectivity mosaic (horizontally interpolated to RR 13-km grid). A standard radar color table is used for the plots.

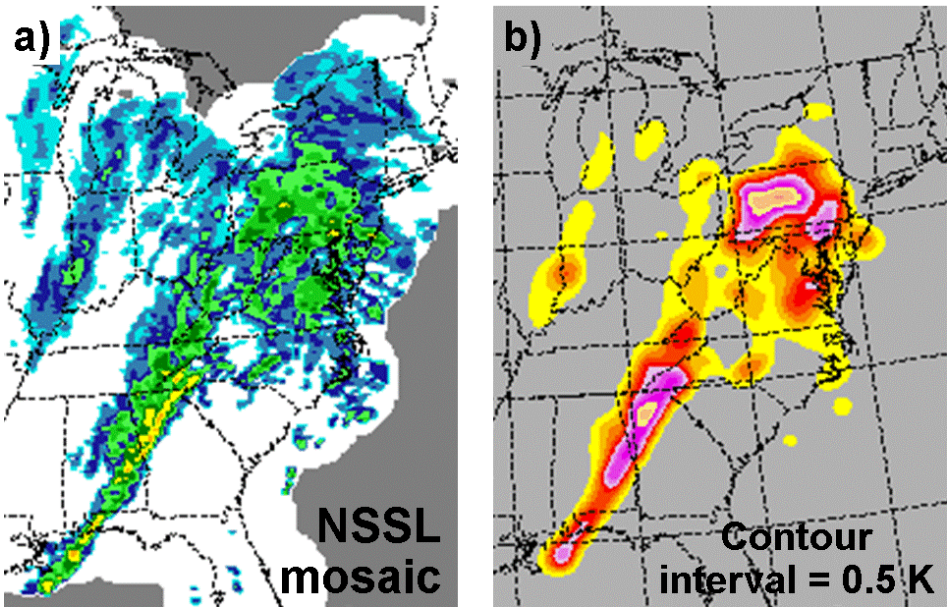

Fig. 7. For 00z 8 January 2007. a) z=3-km radar reflectivity field from NSSL reflectivity mosaic (horizontally interpolated to RUC 13-km grid) plotted with a standard radar color table and b) radar reflectivity derived latent heat temperature tendency field for RUC model level 15 (~850 mb). Color bands are every 0.5 with a maximum of about 5.0 K / 15 min.

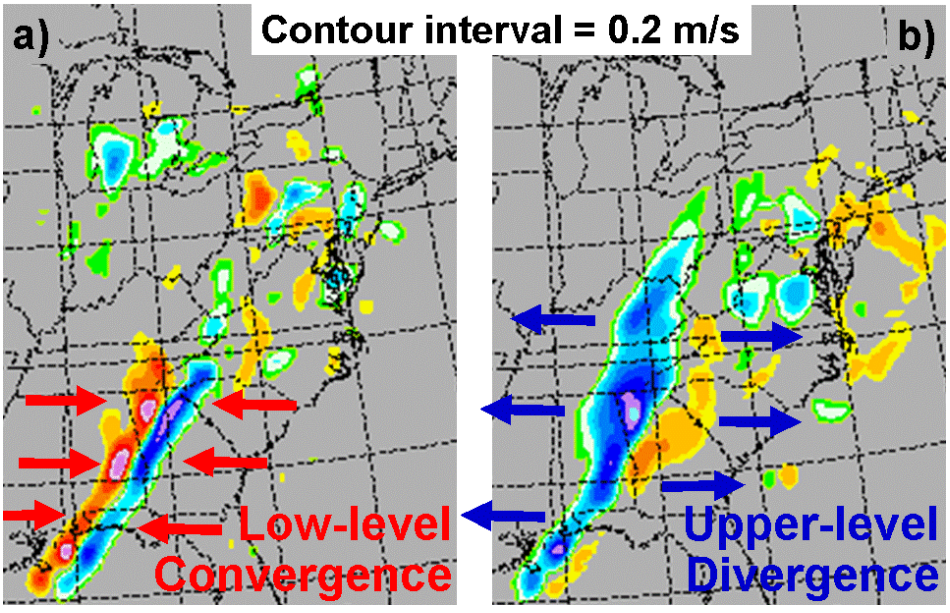

Fig. 8. Also for 00z 8 January 2007, experiment differences (radar assimilation run – no radar assimilation run) in the east-west wind component for a) RUC model level 15 and b) RUC model level 35. Color bands are every 0.2 m/s with warm colors indicating enhanced westerlies in the radar assimilation experiment and cool colors indicating enhanced easterlies. As can be seen by the respective couplets, the radar assimilation induces low-level convergence and upper-level divergence along the squall-line.

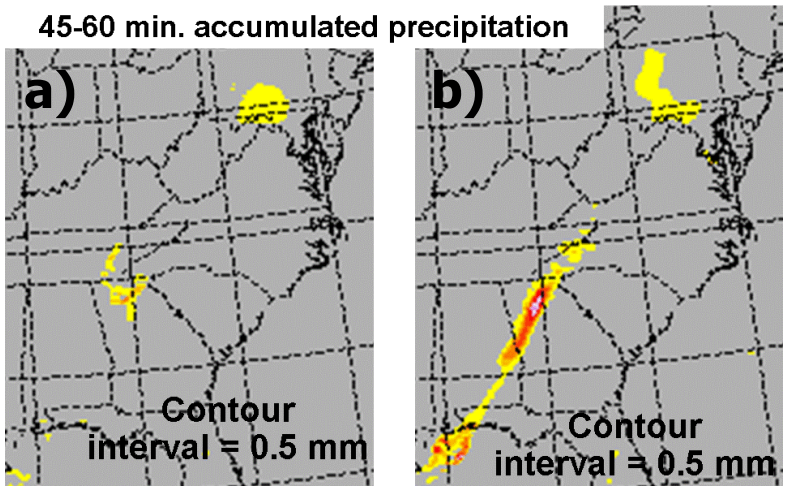

Fig. 9. 1-h forecast (valid 01z 8 January 2007) of 15-min (45 to 60 min.) accumulated total precipitation (explicit + parameterized) for a) the no radar assimilation experiment and b) the radar assimilation experiment. Color bands are every 0.5 mm.

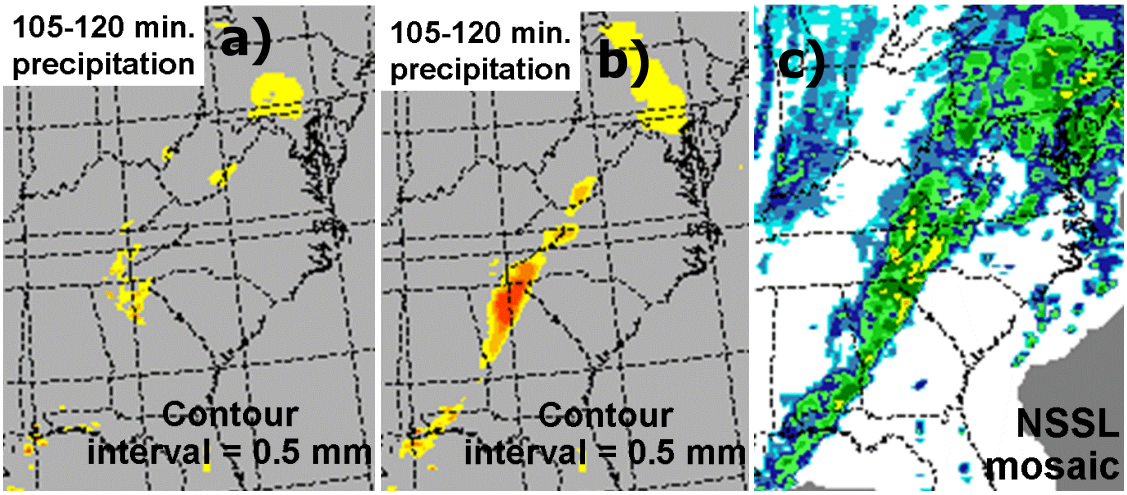

Fig. 10. 2-h forecast (valid 2z 8 January 2007) of 15-min (105 to 120 min.) accumulated total precipitation for a) the no radar assimilation experiment and b) the radar assimilation experiment. Color bands are every 0.5 mm. c) z= 3-km radar reflectivity from NSSL mosaic (horizontally interpolated to RUC 13-km grid) valid 02z 8 January 2007.

Comparison of the forecast precipitation fields (Figs. 10a,b) with the radar image from 02z indicates that the model run with the radar assimilation does a better job predicting precipitation for the areas with strong radar echoes.

5. REAL-TIME TEST CASES RESULTS

Based on the encouraging results from the preliminary tests, the radar assimilation procedure was implemented in a real-time parallel RUC cycle run at GSD in February 2007. Utilizing the real-time feed of hourly radar composite data from NSSL and NLDN lightning data, the radar assimilation algorithm was applied on an hourly basis. Monitoring of the real-time forecasts with the radar assimilation compared to the operational RUC forecasts without the radar assimilation has continued to reveal a short-range (3-h) positive impact in precipitation forecasts. This is clearly evident in precipitation skill-scores for a one-month comparison period shown in Fig. 11. Equitable threat scores for the radar

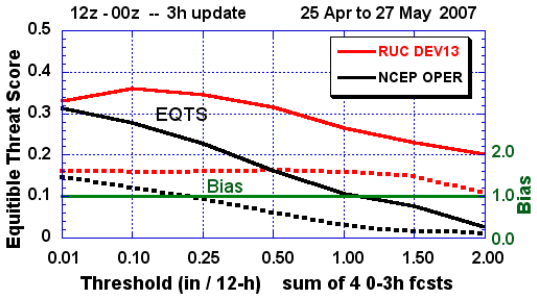

Fig. 11. Effect of reflectivity assimilation on precipitation verification for 12-h periods from 12z to 00z (daytime) for 25 Apr – 17 May (27 cases). For each 12-h verification period, 0-3 hour forecasts from the 12, 15, 18, and 21z cycles are summed. RUC DEV13 indicates the RUC 1-h cycle with the radar assimilation; NCEP OPER indicates the NCEP operational RUC 1-h cycle without the radar assimilation.

assimilation runs remain above 0.2 for all thresholds up to 2.0 inches. Comparable scores for the operational run (no radar assimilation) decrease dramatically to near zero for the higher thresholds. Bias scores are also more favorable for the radar assimilation run, reflecting an improvement over the operational run, which severely underpredicts the higher precipitation amounts.

Specific examples of the improvement from the radar assimilation have been easy to find in the real-time RUC forecasts. Fig. 12 shows a dramatic example of the RUC forecasts from the radar assimilation. The case is dominated by two mesoscale convective systems. The first propagated southeastward from Northern Illinois into central Indiana, before weakening around 12z. The second system developed northwest of the first and was propagating southward across Central Illinois at 12z. The top panel of Fig. 12 shows the RUC 3-h forecast 3-h accumulated precipitation valid 12z 17 July 2007. The middle panel shows the corresponding RUC forecast with the radar reflectivity assimilation and the bottom panel shows the NSSL 3-h estimated precipitation also valid 12z 17 July 2007. As can be seen, the radar assimilation results in a much better RUC 3-h precipitation forecast.

We show a final case from a very high aviation impact day, 10 July 2007. On this day, a squall-line rapidly developed around 18z west of Chicago and propagated across O'Hare airport causing significant delays. Fig. 13 shows a comparison of the 21z verifying VIP levels from MIT/LL and 18z + 3h

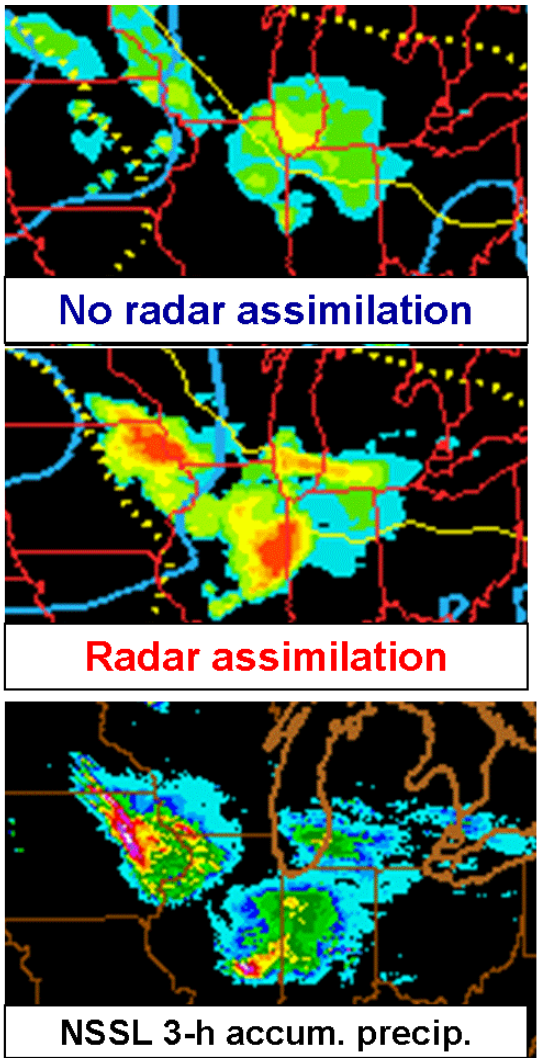

Fig. 12. Sample improvement from radar assimilation as reflected in the new RUC simulated reflectivity field for 3-h forecast valid 00z 25 March 2007. a) observed radar reflectivity, b) RUC forecast with radar assimilation, and c) RUC forecast without radar assimilation.

forecast reflectivities from HRRR runs initialized with 1) the GSD RUC version that had the reflectivity assimilation and 2) the operational RUC version that does not yet have the reflectivity assimilation. While both provide reasonable overall forecasts of the convective evolution, the HRRR forecast initialized from the RUC with the reflectivity assimilation (middle panel) better captured the solid line approaching Chicago O'Hare airport, as well as a number of other convective features (storms in southern Illinois, southwestern Ohio, and Ontario).

6. SUMMARY AND FUTURE PLANS

We are currently using NLDN lightning data within the real-time developmental version of the RUC model run at GSD. The lightning data are converted to proxy reflectivity data using a simple assumed linear relationship. These inferred reflectivity data supplement the NSSL radar reflectivity data. This combined reflectivity field is then used to specify a latent-heating-based temperature tendency that is applied during a diabatic pre-forecast digital filter initialization. This induces convective scale vertical circulations and projects onto both the parameterized and explicit precipitation modules in the RUC, yielding impressive warm season precipitation skill score improvements.

Evaluation of individual case studies indicates significant improvement for convective systems. Comparison of 3-km HRRR forecasts initialized from RUC runs with and without the radar assimilation procedure indicates that assimilation of the radar / lightning data on the 13-km RUC grid often leads to improvements on the nested 3-km domain. It is crucial to note that we have not done specific tests to isolate the impact solely due to the lightning data and the encouraging results shown for the assimilation procedure are almost certainly produced primarily from the radar data. We plan to do a series of tests to isolate the impact from the lightning data both as a supplement and replacement for the radar data. This new assimilation system (with radar data availability only) is in final parallel testing at NCEP and will be a main component of the NCEP RUC upgrade planned for summer 2008.

Much of the work to port this radar / lightning assimilation system to the GSI / RR has been completed and we anticipate real-time testing of this capability within the hourly cycled RR will begin this summer (2008). The availability of Alaskan BLM lightning data (in addition to the NLDN data) will be extremely helpful and we eager to explore the use of lightning data from other networks (Canada, long range networks, etc.). As we transition from the operational RUC to the Rapid-Refresh, the importance of lighting data will increase significantly.

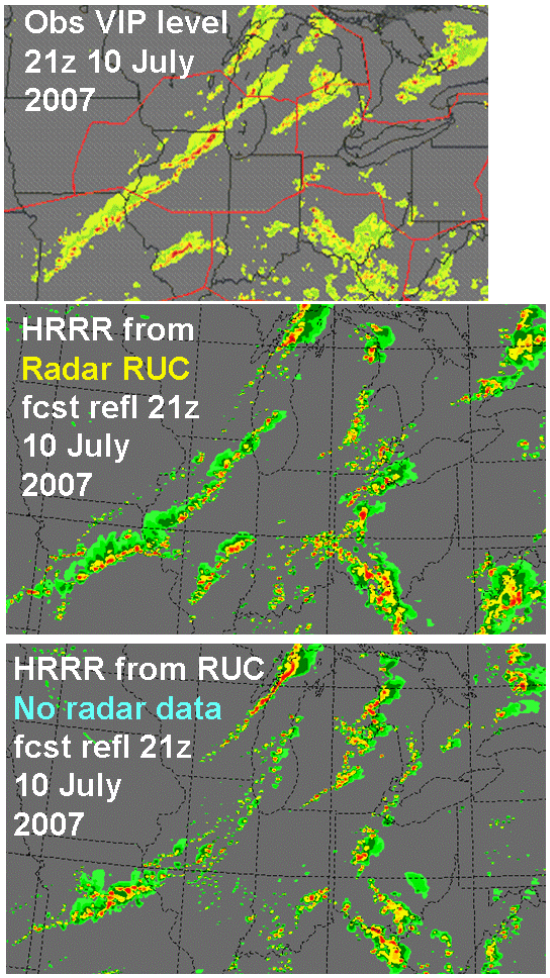

Fig. 13. Comparison of 3-h HRRR forecast reflectivity valid 21z 10 July 2007 – with (middle panel) and without (bottom panel) RUC reflectivity assimilation. VIP level verification is shown in top panel.

7. REFERENCES

Benjamin, S.G., D. Devenyi, S.S. Weygandt, K.J. Brundage, J.M. Brown, G.A. Grell, D. Kim, B.E. Schwartz, T.G. Smirnova, T.L. Smith, and G.S. Manikin, 2004a: An hourly assimilation/forecast cycle: The RUC. *Mon. Wea. Rev.* ,**132**, 495-518.

Benjamin, S.G., G.A. Grell, J.M. Brown, T.G. Smirnova, and R. Bleck, 2003b: Mesoscale weather prediction with the RUC hybrid isentropic / terrain-following coordinate model. *Mon. Wea. Rev.* ,**132**, 473-494.

Benjamin, S.G., D. Kim, and J.M. Brown, 2002: Cloud/hydrometeor initialization in the 20-km RUC with GOES and radar data. Preprints, 10th Conf. on Aviation, Range, and Aerospace Meteorology, Portland, OR, Amer. Meteor. Soc., 232-235.

Benjamin, S., D. Devenyi, T. Smirnova, S. Weygandt, J. M. Brown, S. Peckham, K. Brundage, T. L. Smith, G. Grell, and T. Schlatter, 2006: From the 13km RUC to the Rapid Refresh. *12th Conference on Aviation Range and Aerospace Meteorology*, Atlanta, GA, American Meteorological Society, 9.1.

Benjamin, S., and co-authors, 2007: From the radar enhanced RUC to the WRF-based Rapid Refresh. *18th Conf. Num. Wea. Pred.,* Park City, UT, AMS, J3.4.

Benjamin, S. G., G. A. Grell, J. M. Brown, T. G. Smirnova, and R. Bleck, 2004a: Mesoscale Weather Prediction with the RUC Hybrid Isentropic/Terrain-Following Coordinate Model. *Monthly Weather Review*, **132,** 473-494.

Benjamin, S. G., S. S. Weygandt, J. M. Brown, T. L. Smith, T. Smirnova, W. R. Moninger, and B. Schwartz, 2004b: Assimilation of METAR cloud and visibility observations in the RUC. *11th Conference on Aviation, Range, Aerospace and 22nd Conference on Severe Local Storms*, Hyannis, MA, American Meteorology Society, 9.13.

Benjamin, S. G., D. Devenyi, S. S. Weygandt, K. J. Brundage, J. M. Brown, G. A. Grell, D. Kim, B. E. Schwartz, T. G. Smirnova, T. L. Smith, and G. S. Manikin, 2004c: An Hourly Assimilation/Forecast Cycle: The RUC. *Monthly Weather Review*, **132,** 495-518.

Devenyi, D. and S. Benjamin, 2003: A variational assimilation technique in a hybrid isentropic-sigma coordinate. *Meteor. Atmos. Phys.,* **82,** 245-257.

Devenyi, D., S. Weygandt, T. Schlatter S. Benjamin, and M. Hu, 2007: Hourly data assimilation with the Gridpoint Statistical Interpolation for Rapid Refresh. *18th Conf. Num. Wea. Pred.,* Park City, UT, AMS, 4A.2.

Hu, M., S. Weygandt, S. Benjamin, and M. Xue, 2008: Ongoing development and testing of a generalized cloud analysis package within GSI for initializing Rapid Refresh. *13th ARAM Conf.,* New Orleans, LA, AMS, 7.4.

Huang, X. and P. Lynch, 1993: Diabatic digital-filtering initialization: Application to the HIRLAM model. *Monthly Weather Review*, **121,** 589-603.

Lynch. P. and X. Huang, 1992: Initialization of the HIRLAM model using a digital filter. *Monthly Weather Review*, **120,** 1019-1034.

Thompson, G., R. M. Rasmussen, and K. Manning, 2004: Explicit Forecasts of Winter Precipitation Using an Improved Bulk Microphysics Scheme. Part I: Description and Sensitivity Analysis. *Monthly Weather Review*, **132,** 519-542.

Weygandt, S., S. G. Benjamin, D. Dévényi, J. M. Brown, and P. Minnis, 2006a: Cloud and hydrometeor analysis using metar, radar, and satellite data within the RUC/Rapid-Refresh model. *12th Conference on Aviation Range and Aerospace Meteorology*, Atlanta, GA.

Weygandt, S.S., S.G. Benjamin, J.M. Brown, and S.E. Koch, 2006b: Assimilation of lightning data into RUC model forecasting. *2nd Intl. Lightning Meteorology Conf.* Tucson, AZ

Zhang, J., C. Langston, K. Howard, and B. Clarke, 2006: Gap-filling in 3D radar mosaic analysis using vertical profiles of reflectivity. *12th Conference on Aviation Range and Aerospace Meteorology*, Atlanta, GA.